STUDIA UNIVERSITATIS BABEŞ-BOLYAI, CHEMIA, LIV, 3, 2009

PHOTO-CATALYSTS BASED ON GOLD - TITANIA COMPOSITES

ANCA PETER[a], MONICA BAIA[b], FELICIA TODERAS[b], MIHAELA LAZAR[c], LUCIAN BARBU TUDORAN[d], VIRGINIA DANCIU[e]

ABSTRACT. Porous TiO_2 aerogels with different Au colloidal particles concentrations were synthesized and their functionality to decontaminate the water was evaluated using model pollutants. It was showed that the decrease of noble metal concentration determines a decrease of the composites pore size and specific surface area and of the photo-degradation apparent rate constant. The morphological (porosity, surface area, TEM and TGA) particularities of the synthesized porous composites were also briefly discussed from the perspective of the photo-catalytic results. Since the photodecomposition rate depends on the $[OH]_{surface}$ adsorbed on the surface, additional measurements have been performed.

Keywords: *Au -TiO_2 composite, porosity, TEM microscopy, photo-catalysis, salicylic acid*

INTRODUCTION

TiO_2 photo-catalysis has been improved by numerous investigations in recent years, particularly owing to its application for the complete mineralization of almost all organic contaminants to carbon dioxide, water and inorganic constituents [1, 2]. The advantages of using TiO_2 are its non-toxic nature and stability, but it is also significant that the low rate of electron transfer to oxygen and the high recombination rate of electron-hole pairs limit the rate of organic compounds photo-oxidation on the catalyst surface [3]. Many investigations have reported that the addition transition metals to TiO_2 are two ways to enhance the photo-catalytic reaction rate [3-9]. The noble metals as gold [4, 5], platinum [6, 7] and silver [9] were usually

[a] *North University, Faculty of Science, Department of Chemistry-Biology, 430083, Baia Mare, Romania, peteranca@yahoo.com*
[b] *Babes-Bolyai University, Faculty of Physics, 400084, Cluj-Napoca, Romania*
[c] *National Institute for Research and Development of Isotopic and Molecular Technologies, Donath 71 – 103, RO-400293, Cluj-Napoca, Romania*
[d] *Faculty of Biology and Geology, Electron Microscopy Center, Babes-Bolyai University, 5-7 Clinicilor Str., 400006, Cluj-Napoca, Romania*
[e] *Babes-Bolyai University, Faculty of Chemistry and Chemical Engineering, 400028, Cluj-Napoca, Romania*

used to produce the highest Schottky barriers among the metals, in order to facilitate the electron capture. Moreover, the research studies [10, 11] have demonstrated that the gold particles interact with TiO_2 surface oxygen vacancies (note that on an oxygen vacancy site, two neighbouring Ti atoms are reduced from Ti^{4+} to Ti^{3+}), thus reducing the surface defects.

Due to their very low density, high surface area, translucency or transparency to the visible light and to their microstructure, the TiO_2 aerogels are the preferred materials as supports for noble metals. On the other hand, the photo-catalytic activity of Au-TiO_2 composites has been described as strongly influenced by morphological and structural parameters, such as their structure, surface area, porosity, gold particle size and surface hydroxyl group density [12, 13].

In this paper, we study the photo-catalytic behaviour of a series of Au - TiO_2 composites in the aqueous salicylic acid (SA) oxidation. The goal of this study was to investigate the influence of the Au loading on the photo-catalytic activity of the Au –TiO_2 composites.

RESULTS AND DISSCUTION

Morphology and Structure of the Composites

The morpho-structural characteristics of the Au – TiO_2 composites are presented in Table 1. In columns 2 and 3 of the Table 1 are indicated the gold colloid volumes used to the TiO_2 gels impregnation and gold content, respectively. One observes an increase of the Au content as the colloid volume increases from 20 to 75 ml. By using a volume higher than 75 ml Au colloid, the Au content slowly decreases, probably due to the saturation of the TiO_2 surface with Au particles (Figure 1).

The pore size distribution of the obtained composites is presented in Figure 2 A (a-e). The Au -TiO_2 composites have a porous structure containing pores ranging from 8 to 55 Å, while TiO_2 aerogel contains pores ranging from 20 to 80 Å. So, the Au presence in the composites reduces the composite's porosity. This behaviour was attributed to the insertion of a small amount of gold nano-particles into the pores. This insertion occurs without damaging the pore structure. Similar changes have been reported in the surface structure of porous titania with the insertion / deposition of ruthenium and platinum nano-particles by the sono-chemical method [14, 15]. The decrease of porosity by Au deposition can be observed also by analyzing the pore volume values from Table 1. It is interesting to notice that the porosity decreases with the decrease of Au content (Figure 2B). The B1Au and B2Au composites with similar Au content (0.395 % and 0.397%, respectively) have the major pore size ranging from 35 to 40 Å while B4Au composite with 0.131% Au, which contains predominantly 15 A pores. At low Au concentrations, pores with 20 Å diameters are dominant, whereas composites with high Au content (samples B1Au and B2Au) contain pores with diameters higher than 20 Å.

Table 1. Morpho-structural particularities and photo-catalytic behavior of the studied Au-TiO_2 composites

Au - TiO_2 ID	$V_{Au\ coll.\ sol.}$ (ml)	[Au] (% mol)	S_{BET} (m^2/g)	V_{pore} (cm^3/g)	$[OH]_{surf}$ (mmol/g)	k_{ads} x 10^3 (min^{-1})	k_{photo} x 10^3 (min^{-1})	X (%)
B1 Au	150	0.395	477	0.86	0.56	0.23	10.9	63
B2 Au	75	0.397	450	0.44	0.61	0.24	11	59
B3 Au	40	0.373	332	0.38	0.52	0.12	10.6	52
B4 Au	25	0.131	337	0.95	0.57	0.04	8.1	50
TiO_2	-	-	340	1.08	0.6	0.09	10.1	60

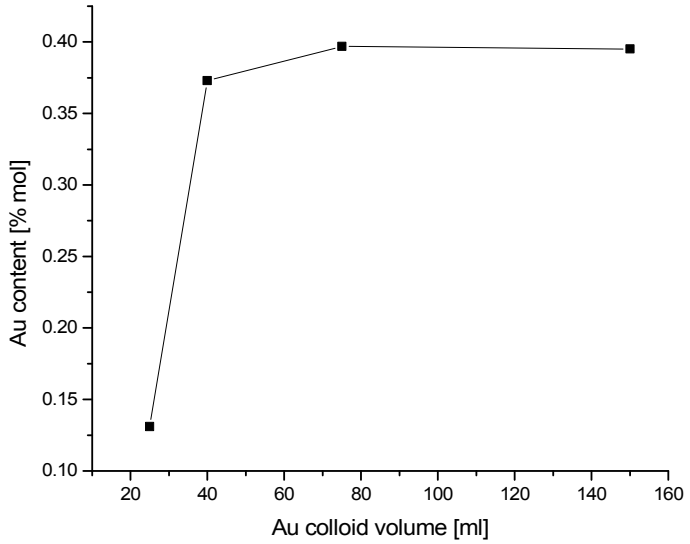

Figure 1. Dependence of Au content on the Au colloid volume used inTiO_2 gel impregnation

The specific surface area BET of the obtained composites increases with Au content (Table 1). These effects have been previously reported for gold supported on MCM-41 and MCM-48 zeolites [16] and for gold supported on alumina and ceria [17], and are explained through the expansion of the porous structure of the support due to of the introduction of gold nano-particles [18].

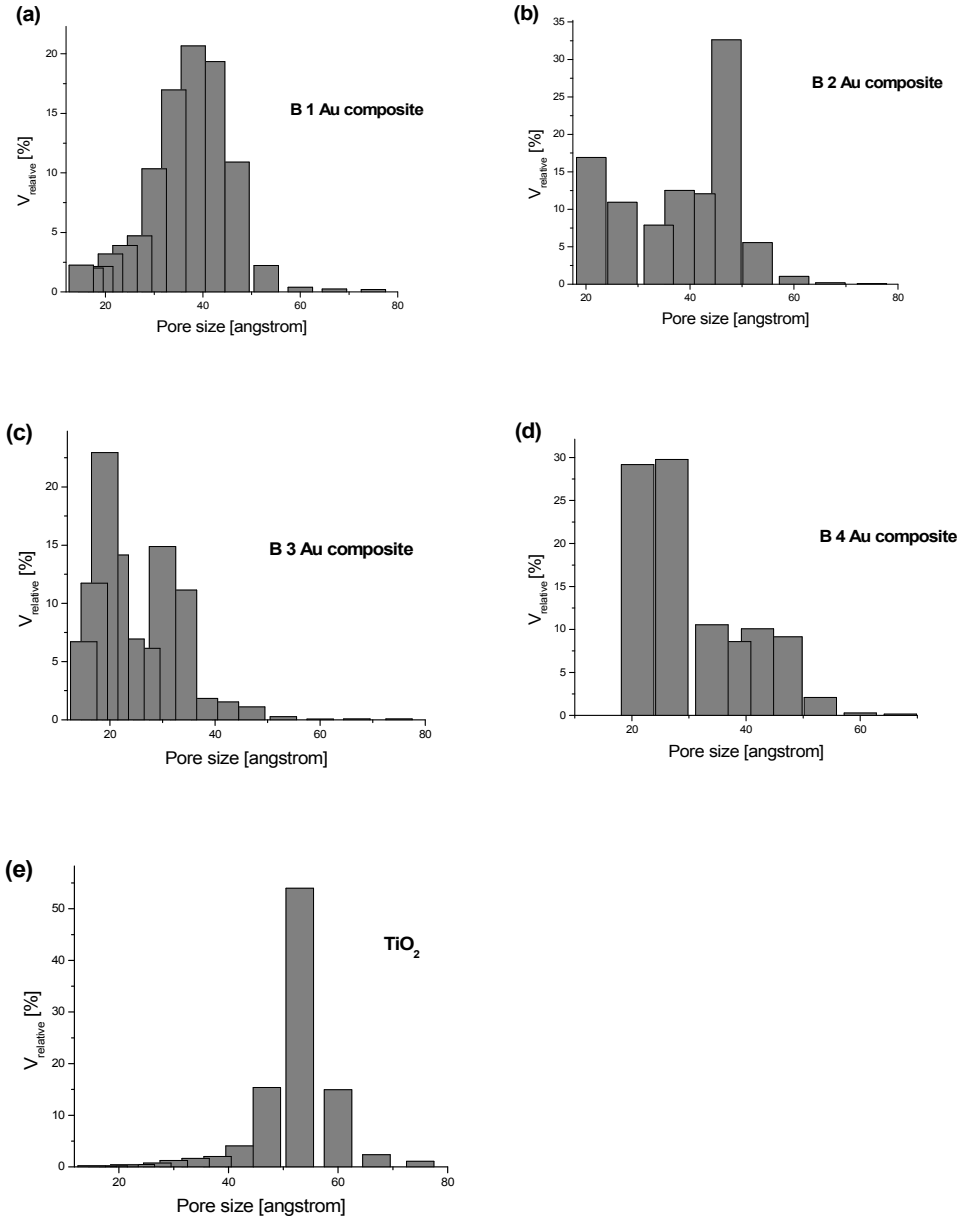

Figure 2A. Influence of the Au loading on the composites pore structure.

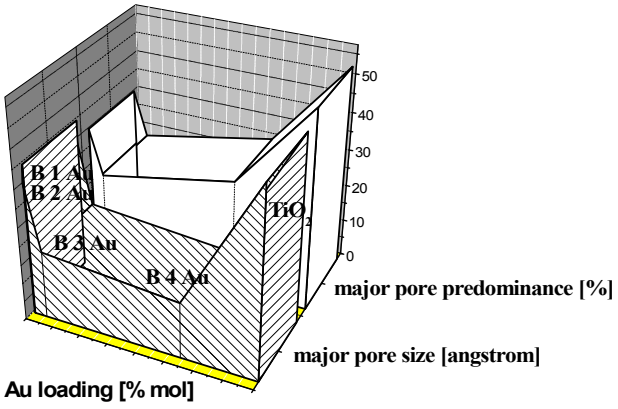

Figure 2B. Variation of major pore size and major pore predominance with Au loadings.

According to TEM pictures analysis, the composite B1Au (Figure 3) has an amorphous TiO_2 structure. The Au particles (dark points) are heterogeneously dispersed on the TiO_2 surface. In some areas, the Au colloidal particles were agglomerate into clusters (indicated by the arrow from Figure 3), while in other regions individual Au particles with a 15 nm diameter (determined from TEM analyses) were detected. The association of Au nano-particles in large clusters reduced the TiO_2 photo-excitation, due to the fact that all its active centres are occupied with Au particles. This behaviour will, subsequently, cause a decrease of the SA photo-degradation rate.

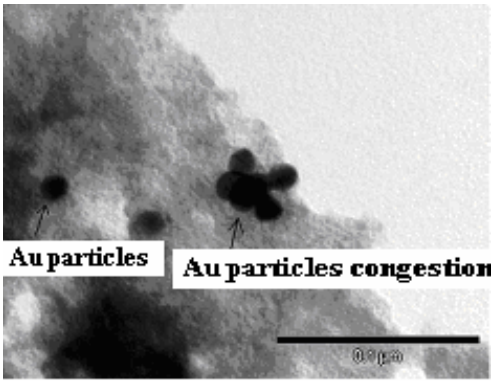

Figure 3. TEM image of the B1Au composite (bar 100 nm).

In Figure 4 presents the Au -TiO_2 composites weight decrease after heat treatment at temperatures increasing from 25 to 500^{0}C.

The weight loss at t < 200^{0}C is due to the first dehydration step, resulted from physically adsorbed water, and the elimination of the ethanol traces [19]. It can be observed that the mass loss increases with decrease of the Au content. This is explained by the fact that the Au nano-particles from TiO_2 surface inhibit the network shrinkage in thermal treatment. At 250-300^{0}C, a second dehydration step resulted from structural / ligand water and thermal decomposition of the un-reacted titania precursors, takes place. Again, at this stage, the mass loss increases with decrease of the Au content. This is explained by the fact that the higher number of Au nano-particles from TiO_2 surface stabilize the aerogel network, by forming a metal skeleton around the TiO_2 structure. Moreover, at temperatures higher than 300^{0}C, the aerogel begins to become crystalline. By comparing the weight loss of the TiO_2 and Au -TiO_2 composites, one observes that the TiO_2 network is more stable than the composites network. The weight loss in the case of TiO_2 aerogels is lower than that observed for the composites.

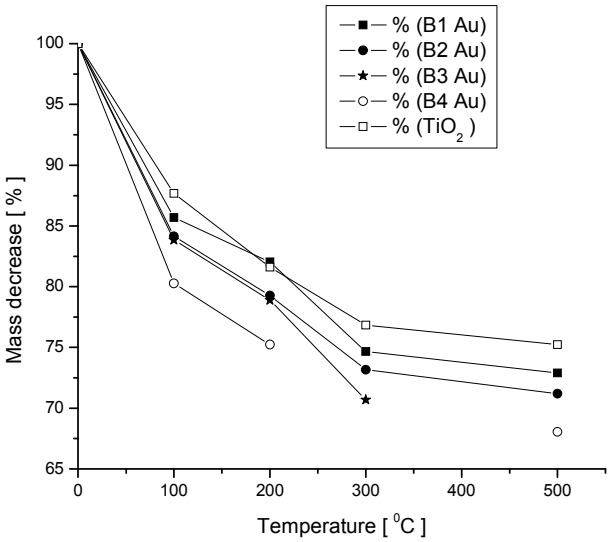

Figure 4. Influence of the Au loading on the thermal behavior of the Au-TiO_2 composites.

Catalytic Activity

In Table 1, there are presented some catalytic parameters (salicylic acid adsorption and photo-degradation apparent rate constants and photo-degradation efficiency) which are determinated for the SA photo-decomposition process. The adsorption constants were calculated from the slope of the plot

ln (Q_t) *vs.* time (Q_t – current adsorbed quantity) after applying a linear fit [20]. The photodecomposition rate constants were obtained from the slope of the plot ln (C_0/C) *vs.* time after applying a linear fit [21, 22]. The photo-degradation efficiency was calculated with the following equation:

$$X\ (\%) = (C_0 - C) / C_0 \times 100 \qquad (1)$$

where: C_0 – SA initial concentration, C– SA concentration after 150 minutes iradiation [23].

The more intense adsorption of SA occurs on B1Au and B2Au composites with the highest Au content (Table 1 and Figure 5). The adsorption rate constants decrease with decrease of the Au loading, in the same manner as the specific surface area and pore volume. Moreover, the $[OH]_{surface}$ is relatively high for those two composites, except for the B4Au sample which has the highest $[OH]_{surface}$. Even if the pore volume and $[OH]_{surface}$ of B4Au composite are highest than those of the other composites, the adsorption rate constant is very low. This is explained by the fact that the B4Au composite contains, in the major preponderance, pores smaller than 20 Å diameter (micro-porous structure) which do not permit the penetration of the SA molecules having a higher surface area (35.52 $Å^2$), due to the steric impediment [24]. So, in this case SA adsorption and photo-decomposition take place only on geometric surface and not in the real surface. This observation is available also for the TiO_2 aerogel and shows that the adsorption intensity is deeply influenced by the specific surface area and pore size.

The SA photo-degradation rate constants vary with Au loading in the same manner as the adsorption constants (Table 1 and Figure 5). The SA photo-degradation on B1Au, B2Au and B3Au composites occurs with a higher rate, due to the fact that SA adsorption on these composites was more intense. The SA photo-degradation apparent rate constants increase with the specific surface area, pore size and $[OH]_{surface}$. In B1Au and B2Au composites, pores of about 40 Å are predominant, thus the SA molecules may easily get into the composite network, increasing the SA photo-degradation rate.

By comparing the relationship between Au loading and photo-degradation rate constant in the case of B2Au and B4Au composites, one observes that whereas the Au content increase by almost three times, the photo-degradation rate constant increase by 1.35 times. This indicates a non-linear dependence of photo-degradation rate on Au loading on the composites and challenges to new researches in order to establish that this dependence is kept up for Au loadings higher than 0.397%.

The photo-degradation efficiency (Table 1) decreases with the decrease of the adsorption and photo-degradation rate constants and is influenced also by the specific surface area, pore size and $[OH]_{surface}$, which, subsequently, are induced by the Au loading.

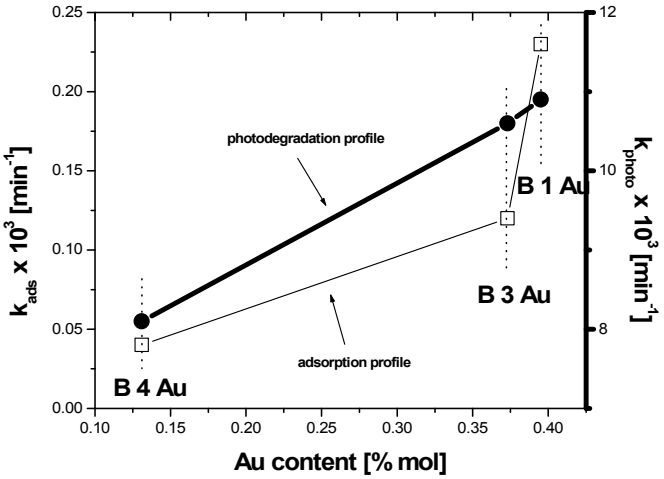

Figure 5. Influence of Au loading on SA adsorption and photo-degradation rate constants (B 1 Au – 0.395% Au, B 3 Au – 0.373% Au, B 4 Au – 0.131% Au)

CONCLUSIONS

Au – TiO_2 composites with different Au loadings were prepared and characterized by nitrogen adsorption-desorption method, TEM microscopy and thermo-gravimetric analyses. Additionally, the OH group's concentration was measured. The catalytic activity of the obtained composites was tested in the SA photo-degradation process.

- The pores size varies inversely proportionate with the Au loading.
- The specific surface area, SA adsorption and photo-degradation rate constants vary proportionate with Au loading.
- The SA adsorption and photo-degradation rates are deeply influenced by the pore size and specific surface area of the Au-TiO_2 composites.

EXPERIMENTAL SECTION

Composites preparation

At first, the TiO_2 gels were prepared by sol-gel method. The TiO_2 sols were obtained by mixing titanium-isopropoxide (IV) (Merck, 99.9%), with anhydrous ethanol (Fluka, 99.8%), ultra pure water and nitric acid reagent (Merck, 65%) as catalyst. The molar ratio of reactants was: $[Ti(OC_3H_7)_4]:[H_2O]:[C_2H_5OH]:[HNO_3]$ = 1:3.675:21:0.08.

The transparent TiO_2 gels were kept for 3 days in a gold colloidal solution, obtained by $HAuCl_4$ 10^{-3} M (Merck, 99.8%) reduction with sodium citrate 38,8 x 10^{-3} M (Merck). The colloidal solution volumes used for TiO_2 gel impregnation were between 25-150 ml (Table 1).

The obtained Au – TiO_2 gels were supercritically dried using liquid CO_2 in a SAMDRI – 790 A (Tousimis) dryer (T = 40 ^{0}C and p = 1400 psi). The composite aerogels were transparent, with a violet nuance. The gold contents for the obtained composites are presented in Table 1.

Characterisation Techniques

The surface area and the pore volume of the as-prepared composites were determined by the Brunauer-Emmett-Teller (BET) method. A Sorptomatic, Thermo Electron Corporation system coupled with a Flatron L 1718S computer system was used. The partial pressure range for surface area calculation was $0.05 < P/P_0 < 0.3$. The nitrogen adsorption was carried out at 77 K. Before each measurement, the composites were degassed at p = 0.5 Pa and T = 333 K for 2 h.

A transmission electron microscope (TEM) Jeol JEM 1010 operating at an accelerating voltage of 100 kV was employed to obtain bright field images. Au particle sizes were measured from images using SIS software after calibration. 400 mesh cooper grid covered with a plain carbon film, obtained by vacuum evaporation on freshly cleaved mica, were used to support a drop of ultrasonic dispersed composite powder in distilled water. The TEM images were recorded with a MegaView III CCD camera.

The thermo-gravimetric analyses were performed using a Thermal Analysis System Mettler Toledo with a thermo-gravimetric cell TGA / SDTA 851 (heating rate 5^{0}C / min, in nitrogen flow) and a thermal analysis cell DSC 822.

The $[OH]_{surface}$ on the TiO_2 aerogels was determined by spectro-photometrical evaluation of the Fe (III) acetyl-acetonate concentration in toluene solution after its partial coupling with $[OH]_{surface}$ (reaction 1) [25].

$$(3\text{-}x)(S\text{–}\ OH) + Fe(acac)_3 \rightarrow (S - O)_{3\text{-}x}Fe(acac)_x + y(Ti_S - OH) + (3\text{-}x)Hacac \quad (1)$$

where: S - aerogel surface, Hacac- pentane-2,4-dione, solvent – toluene.

The concentration of gold in all composites was determinated using an FAAS 800 Flame Atomic Adsorption Spectrometer. The sample preparation consists in the chemical treatment with 5 ml of acid mixture (HNO_3 37%: HF = 4:1 volume proportion). The mixture was homogenized and brought to 25 ml volumetric flask with distilled water and than filtered

Catalytic Activity

The adsorption properties and the photocatalytic activity of the Au -TiO_2 composites was established from the adsorption and photo-oxidation rate of salicylic acid used as a standard pollutant molecule [26]. In all adsorption and photo-oxidation processes 0.05 g composite was used. The decrease in

salicylic acid concentration (C_0 = 5.25 x 10^{-4} M for all investigated composites) was monitored by UV-Vis spectroscopy (λ = 297 nm). The composites immersed in salicylic acid solution were irradiated with a medium pressure Hg lamp HBO OSRAM (500 W). A Teflon photochemical cell with quartz window (S = 12 cm^2) and a volume of 8 ml was also used. The distance between the photochemical cell and the lamp was about 30 cm. The working temperature was of 20-22^{0}C and the solution pH was 5.3. Before the UV irradiation as well as before the UV-Vis measurements, the cell with the SA solution and composite was kept in dark for 30 min in order to achieve the equilibrium of the SA adsorption-desorption process [15]. One should emphasize that throughout the photodecomposition process no shift of the UV band located at 297 nm was observed and no other new absorption band occurred.

ACKNOWLEDGMENTS

This research was supported by a TD No. 44 / 2006 project.

REFERENCES

1. F.B. Li, X.Z. Li, *Appl. Catal. A: General* , **2002**, *228,* 15.
2. M.R. Hoffmann, S.T. Martin, W.Y. Choi, *Chem. Rev*., **1995**, *95*, 69.
3. A. Linsebigler, G. Lu, J.T. Yates, *Chem. Rev.,* **1995**, *95,* 735.
4. C.Y. Yang, C.Y. Liu, J. Chen, *J. Colloid. Interf. Sci.,* **1997**, *191*, 464.
5. C.Y. Yang, C.Y. Liu, X. Zheng, *Colloid. Surf. A*, **1998**, *131*, 271.
6. A. Sclafani, L. Palmisana, G. Marci, *Sol. En. Mater. Sol C*, **1998**, *51*, 203.
7. J.C. Yang, Y.C. Kim, Y.G. Shul, *Appl. Surf. Sci*., **1997**, *121/122*, 525.
8. W. Choi, A. Termin, M.R. Hoffmann, *J. Phys. Chem.,* **1998**, *98,* 13669.
9. P. Falaras, I.M. Arabatzis, T. Stergiopoulos, M.C. Bernard, *Intern. J. Photoen.,* **2003**, *5*, 123.
10. M.S. Chen, D.W. Goodmann, *Topics in Catal.*, **2007**, *44, 1-2,* 41.
11. A. Kolmakov, D.W. Goodmann, *Catal. Lett.*, **2000**, *70,* 93.
12. X. Chen, S.S. Mao, *Chem. Rev*., **2007**, *107,* 2891.
13. S. Sakthivel, M.C. Hidalgo, D.W. Bahnemann, S-U Geissen, V. Muguresan, A. Vogelpohl, *Appl. Catal. B*, **2006**, *63*, 31.
14. N. Perkas, Z. Zhong, L. Chen, M. Besson, A. Gedanken, *Catal. Lett.*, **2005**, *103*, 9.
15. N. Perkas, D. Minh Pham, P. Gallezot, A. Gedanken, M. Bessot, *Appl. Catal. B,* **2005**, *59*, 121.

16. Z. Kónya, V.F. Puntes, I. Kiricsi, J. Zhu, J.W. Ager, M.K. Ko, H. Frei, P. Alivisatos, G.A. Somorjai, *Chem. Mater*, **2003**, *15*, 1242.
17. M.I. Dominguez, M. Sanchez, M.A. Centeno, M. Montes, J.A. Odriozola, *Appl. Catal. A,* **2006**, *302*, 96.
18. M.A. Centeno, M.C. Hidalgo, M.I. Dominguez, J.A. Navió, J.A. Odriozola, *Catal. Lett.,* **2008**, *123*, 198.
19. S.A. Selim, Ch.A.Philip, S. Hanafi, H.P. Boehm, *J. Mat. Sci.*, **1990**, *25 (11),* 4678.
20. S.M. Ould-Mame, O. Zahraa, M. Bouchy, *Inter. J. Photoen.*, **2000**, *2*, 59.
21. W. Lee, H-S. Shen, K. Dwight, A. Wold, *J. Sol. State Chem.,* **1993**, *106 (2)*, 288.
22. J. Papp, H. S. Shen, R. Kershaw, K. Dwight, and A. Wold, *Chem. Mater.,* **1993**, *5(3)*, 284.
23. N.A. Laoufi, D. Tassalit, F. Bentahar, *Global Nest Journal,* **2008**, *10(3)*, 404.
24. http://www.chemspider.com/331#suppinfo.
25. J.A. Rob van Veen, F.T.G. Veltmaat, G. Jonkers, *J. Chem. Soc.*, *Chem.Commun.*, **1985**, 1656.
26. M. Tomkiewicz, *Catal. Today,* **2000**, *58*, 115.